Non – proprietary ultra-high-performance concrete with recycled glass powder

Bijaya Rai[a], Kay Wille[b]

[a]Ph.D. student, Department of Civil and Environmental Engineering, University of Connecticut
261 Glenbrook Road, Unit 3037, Storrs, CT 06269-3037, Email: bijaya.rai@uconn.edu, corresponding author
[b]Associate Professor, Civil and Environmental Engineering, University of Connecticut

Abstract

This research emphasizes the development and material characterization of non-proprietary ultra-high-performance concretes (UHPC) using recycled glass powder (RGP) and other suitable local available materials, found in the New England area in the United States. About 10 UHPC pastes and 12 fiber reinforced UHPCs were investigated. The results were compared to two commercial UHPC mixtures, available in the United States. This research showed that UHPC with RGP can be designed to achieve compressive strength of 156 MPa (22.6 ksi) to 178 MPa (25.8 ksi) without the use of special treatment, at current material cost of about US$550/m^3 without fibers and in between US$800 to US$1140/m^3 with the use of fibers available in the US.

Keywords: ultra-high-performance concrete, non-proprietary, recycled glass powder, cost.

1. Introduction

Recycled glass powder (RGP) is an environment friendly supplementary cementitious material (SCMs) (Omran et al. 2018). The RGP used here is 100% post-consumer recycled glass, and its local availability reduces the transportation cost and fuel consumption (Urban Mining 2019; Urban Mining Northeast 2020; Kaminsky et al. 2020). Recycled glass has been used in UHPC as SCMs (Soliman and Tagnit-Hamou, 2016) as well as aggregates (Nancy A. Soliman and Tagnit-Hamou 2017). It can substitute fly ash (FA) in case of its limited availability. It can also be used as partial cement replacement (Soliman and Tagnit-Hamou 2016; Vaitkevičius et al. 2014).

RGP constitutes more than 70% of amorphous silica (Tohoué Tognonvi 2018). When it reacts with the pore solution in concrete it forms calcium silicate hydrate (CSH). Its smaller particle size helps to control and decrease the alkali silica reaction (ASR) (Dyer and Dhir, 2001).

ASTM C 1866 (ASTM C1866) distinguishes between two types of glass power: type GS (Vitro ACAS Grades) used to make beverage containers and plate glass windows, and type GE (Vitro VCAS Grades) used to make fiberglass reinforcements. Type GS recycled glass powder was used in this research.

2. Research approach

2.1. Research outline

Figure 1 summarizes the overall research, which is divided into two parts: (a) UHPC paste investigations, and (b) Investigation of fiber reinforced UHPC.

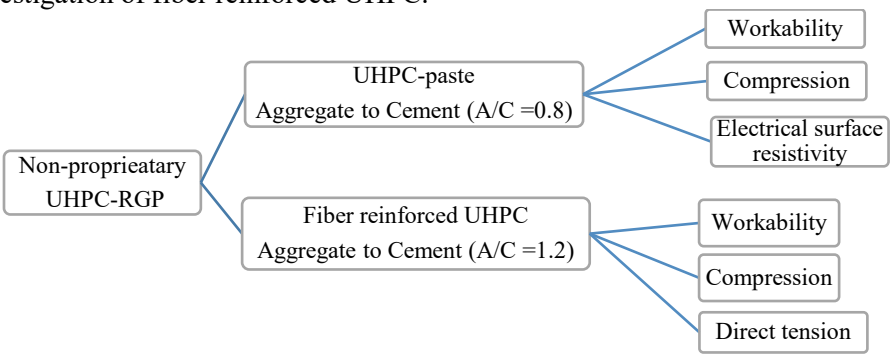

Figure 1: Overall research outline

3. Properties of material constituents

3.1 UHPC constituents

Ordinary Portland cements, type I/II (C I/II) and type II/V (C II/V**)** were selected for their low C_3A content of less than 8% as per recommendation (Sakai et al. 2008). The C_3A content was 7% and 4% for C I/II and C II/V, respectively. Both cements satisfied ASTM C150. Grey silica fume (SF) was selected based on median particle size (D_{50} = 0.5µm**)** and low carbon content (0.3%). The recycled glass powder of type GS was used based on its local availability and its favorable particle size (D_{50} = 9.4µm**)** which filled the particle size gap between SF and cement. Only one type of aggregate, basalt sand (B), with a maximum particle size of 1.18 mm and sieved to follow the modified Andreasen & Andersen (A&A) curve was included in this research. Regarding fiber reinforcement, smooth straight, round steel fiber of 13 mm in length and 0.2 mm in diameter, was used. The summary of UHPC ingredients is presented in the **Table 1.**

Table 2– Summary of UHPC ingredients

Ingredients	Properties	Size
OPC type I/II & II/V	Moderate fineness, low C_3A, high $C_3S + C_2S$	10-20µm
Undensified grey silica fume	Low carbon content	0.2-1µm
Recycled glass powder	Type GS	D_{50} = 9.4µm
Basalt sand	high strength & low water absorption	Less than 1.18 mm
Superplasticizer	High range water reducer	
Steel fiber	Smooth and straight	13mm length/ 0.2mm diameter

As per recommendation (Wille and Boisvert-Cotulio 2015), the mix proportions of the reference UHPC paste in this research are shown in **Table 3 ,** using a weight ratio of PC:SF:SCM=1:0.25:0.25, aggregate to cement ratio by weight (A/C) of 0.8 and aggregate to powder ratio (A/P_o) of 0.53, solid content of HRWR to cement ratio of 0.011, and using local materials available. The cost and carbon footprint (*CFP*) of the paste is calculated per m^3 based on the data obtained from supplier for each ingredient. Commercial UHPCs were mixed as per the instructions from the supplier.

Table 4: – Reference UHPC paste design

Material	ID	amount		$cost_p$	CFP_p
		kg/m³	%	US$/m³	kg/m³
Cement	**C II/V**	913	38.5	141	597
Silica fume	**SF**	228	9.6	154	3.88
Recycled glass powder	**RGP**	228	9.6	35.2	14.2
Basalt sand	**B**	34.0	1.4	170	5.23
HRWR	**HRWR**	747	31.5	27.6	0.0
Water		217	9.3	0.0	0.0
Total				**527**	**620**

Note: W/C = 0.25, A/P_o = 0.53, A/C = 0.8, spread = 260 mm, $f'_{c,Np}$ = 161±8.5 MPa (23.3±1.23 ksi).

3.2 Particle packing analysis

The particle size distribution (PSDs) of SF, RGP and cements were obtained from the suppliers while basalt was sieved and proportioned in the lab to follow the modified Andreasen & Andersen (A&A) curve with a q-value of 0.37 for optimum packing density (Brouwers and Radix 2005). UHPCs were adjusted to follow the modified A&A with a q-value = 0.22 as per recommendation from (Yu 2015; Hunger 2010). The PSDs of the UHPC ingredients and UHPC matrices are presented in **Figure 2.**

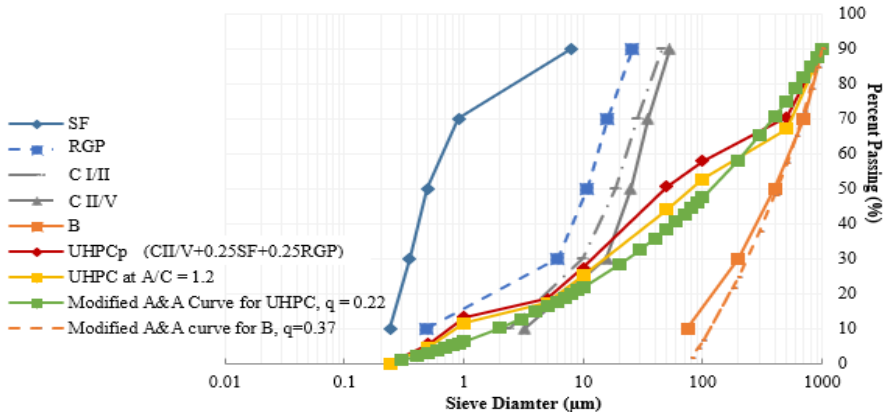

Figure 3: Summary of particle size distributions

4. Testing and sample preparation

4.1 UHPC mixing

All UHPCs were mixed using a rotary Hobart mixer of 20-quart capacity. This mixer provides a bi-rotary mixing technology at three different mixing speeds. All mixes were mixed following the UHPC mixing procedure (Wille et al. 2011). First, SF and aggregates were mixed for five minutes at speed one (107 rpm) to break down potential agglomerations. RGP and PC were added, and all constituents were mixed dry for five more minutes at same speed. Water with one third of HRWR was added first and then the left-over HRWR. During adding water and HRWR, the speed of the rotating blade was maintained at speed one. Then, speed of the mixer was raised to speed two (198 rpm) until it started to turn over, followed by continuous mixing up to five more minutes before casting the UHPC matrix or adding fibers at reduced speed one. In case of fiber addition, the mixer ran for two more minutes to make sure the fibers are sufficiently well dispersed.

4.2 Workability testing

Workability of the UHPCs were evaluated following ASTM C 230/230M (ASTM C230) using standard flow cone (**Figure 3(a)**). Special emphasis was placed on keeping the spread cone and the base plate at a similar humidity for each test.

4.3 Sample preparation

Immediately after the spread test, samples were cast for the different tests. Three 2 in cube specimens were prepared for the compression test using 2 in brass cube molds (**Figure 3(b)**). Five dog bone shaped specimens were prepared for direct tension. Dog bone samples were cast in layers and were reinforced with steel meshes at both ends to facilitate tensile failure in the middle section of the specimen. Each specimen had a constant cross-sectional area of 1 in^2 (645 mm^2) and a gauge length of 3.14 in (80 mm).

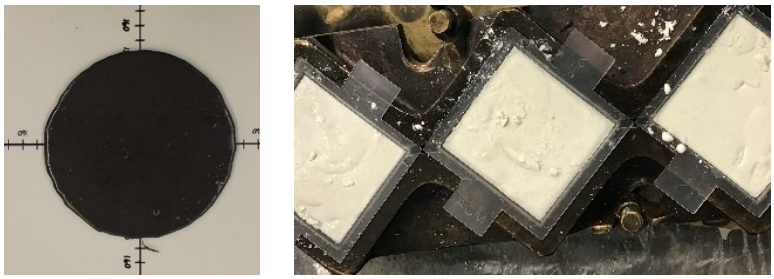

(a) Spread test (b) Cubes preparation

Figure 3: Spread and sample preparation

In addition, two 3 in x 6 in cylinders were cast for testing the UHPC's electrical surface resistivity. All the cube molds, cylinders and dog bone molds were vibrated for consolidation for 2.5 minutes at a frequency of 3.5 Hz. About 30 minutes after pouring the concrete, the molds were covered with plastic to avoid the evaporation of water from the specimens. The samples were demolded after 24 hours and cured at 20°C and 95% of relative humidity.

4.4 Test methods

4.4.1 Compressive strength test

Three 2 in concrete cubes were used for compression testing (**Figure 4(a)**). The cubes were polished before testing to minimize stress concentrations during compression testing. A straight edge was placed on the prepared loading face of the cube and a feeler gauge was used to test the quality of planeness. If the gauge was able to pass under the straight edge, the cube was insufficiently plane and were polished again. At 28th day of casting the compression test was performed as per ASTM C109/C109M-16a (ASTM C109) at the loading rate of 30,000 lb/min.

4.4.2 Direct tension test

For each series, five dog bone specimens were prepared. The direct tension test set up was designed based on Wille et al., 2014 (Wille et al. 2014). **Figure 4(b)** shows the enhanced test setup for the direct tension test and the dog bone specimen used for the test. The holders at the top and bottom of the specimen were

designed to allow three degrees of rotational freedom, thus, to minimize the introduction of bending stresses. Two LVDTs were attached on both sides of the specimen to measure the extension. Enhanced consistency in the obtained load versus displacement curves validated the suitability of this test setup. A 400 kips hydraulic test machine was used to carry out the test.

4.4.3 Electrical surface resistivity

The electrical surface resistivity tests were used to determine the permeability of concrete in accordance with AASHTO TP95 (AASHTO-T95). It is a non-destructive test method and therefore can be used to monitor the change in surface resistivity with the development of pore-structure of the concrete over time. Since the pore-structure densifies with aging of the concrete increase in resistivity over time is expected. **Figure 4(c)** shows the electrical surface resistivity test up.

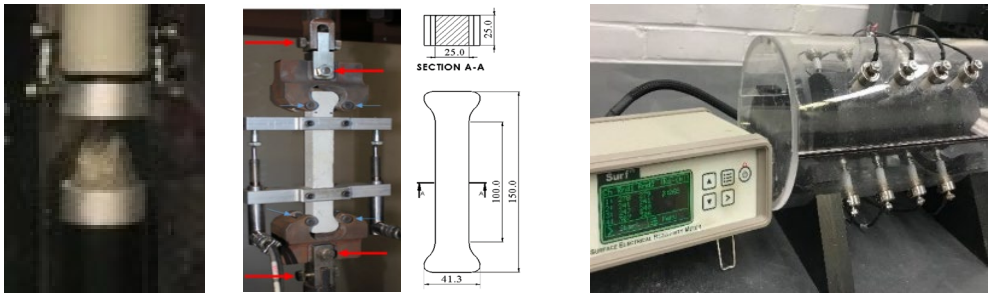

(a) Compression test (b) Direct tension test (c) Electrical surface resistivity test

Figure 4: Different test setups

5. Test results and discussion

5.1. Spread and compressive strength

The UHPC paste using CII/V + RGP (**Table 5**) achieved a spread of 260 mm. The same UHPC paste with FA as replacement for RGP achieved a spread of 288 mm even with lower W/C of 0.24. Using CI/II and RGP with slightly higher W/C of 0.26 resulted in a spread of 228 mm which is attributed to the higher C_3A content. All the pastes contained basalt aggregates with A/C=0.8 to facilitate the breakdown of potential agglomerations of the fine powders. All the UHPC pastes achieved compressive strengths greater than 150 MPa (22 ksi). The results for the UHPC pastes are presented in the **Table 6** below:

Table 7: Comparison between two UHPC pastes

Results	**CII/V+FA C (W/C=0.24)**	**CII/V+RGP (W/C=0.25)**	**CI/II+RGP (W/C=0.26)**
Spread	288 mm	260 mm	228 mm
Compr. strength (f'_c)	164±7.6 MPa (23.8±1.10 ksi)	161±8.5 MPa (23.3±1.23 ksi)	157.5±3.02 MPa (22.8±0.437 ksi)

Table 8 shows that RGP requires more water than FA C due to particle size (D_{50} = 9.4µm vs 11.3µm) and morphology (angular vs round) for RGP vs FA, respectively. **Table 9** also shows that the replacement of FA by RGP lead to similar compression strength results (164 MPa vs 161 MPa). By increasing the amount of aggregates to an A/C = 1.2 and adding fibers of 1.5 vol.% to the UHPC pastes, fiber reinforced UHPC with RGP were obtained. Their compressive strength and spread test results are presented in **Table 4** below.

Table 4: Comparison among fiber reinforced UHPCs (with CI/II and CII/V), A/C = 1.2, V_f=1.5%

Results	UHPC – CI/II			UHPC – CII/V
W/C	**0.26**	**0.27**	**0.30**	**0.26**
Spread	155 mm	195 mm	248 mm	266 mm
Compressive strength (f'_c)	161±0.63 MPa (23.3±0.09ksi)	161±4.15 MPa (23.3±0.60 ksi)	156±0.85 MPa (22.6±0.12 ksi)	178±4.42 MPa (25.8±0.64 ksi)

Table 4 shows that the use of CII/V cement resulted in a better workability behavior and increased compressive strength with a lower W/C as compared to UHPC with CI/II.

However, due to the better availability of CI/II in comparison to CII/V it was decided to carry out further investigation on its tensile behavior with a W/C = 0.30 and fiber volume fractions of 1.0%, 1.5%, and 2.0%. The tensile behavior of the fiber reinforced UHPCs are presented below in the section **5.2.1.**

5.2. Tensile behavior

5.2.1 Direct tension test results

Figure 5(a) shows the consistent tensile stress versus strain behavior of all specimens of one series and its average stress versus strain curve. Plotting the average curves of each series allows for the direct comparison of the UHPC with a fiber volume fraction of 1.0%, 1.5% and 2.0% (**Figure 5(b)**). The tensile strength of the fiber reinforced UHPC with RGP increased from 9 MPa (1.3 ksi), to 11 MPa (1.6 ksi) and to 15 MPa (2.2 ksi) by the increase in fiber volume from 1.0% to 1.5% and to 2.0%, respectively. It can also be seen that a more pronounced strain hardening behavior is achieved with the increase in fiber volume. Especially, UHPC with V_f = 2.0% showed a good ductile behavior with multiple hair line cracks and distinct strain hardening before major crack opening. When this result is compared to a commercial UHPC with V_f = 2.0%, similar behavior is shown (**Figure 5(c)**). The commercial UHPC gained tensile strength up to 14 MPa (2.03 ksi).

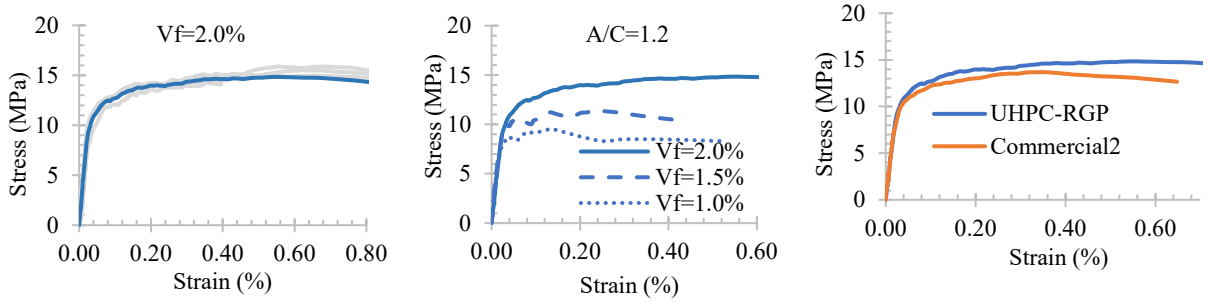

(a) Example of consistent data (b) Effect of different V_f (c) Versus Commercial UHPC

Figure 5: Direct tension test results

5.2.2 Electrical surface resistivity

Figure 6 shows the electrical surface resistivity test results of the UHPC pastes since inclusion of fibers in the UHPC affect the test results significantly. The test results are very promising considering that a low permeability concrete is defined by an electrical resistivity value of more than 27 k-ohm-cm as per ASHTO

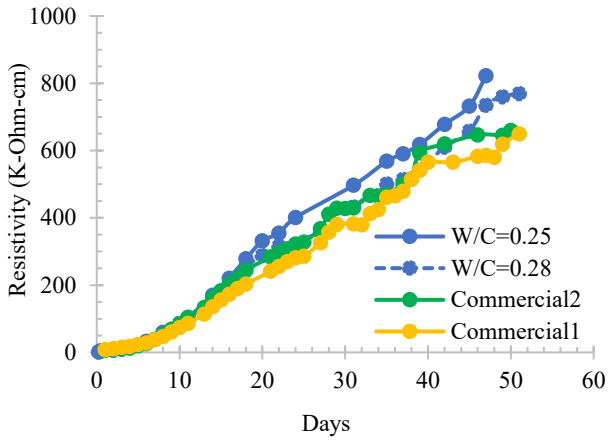

Figure 4: Electrical surface resistivity test results

TP95. This has been achieved in early age and significantly outperformed with the aging of the UHPCs. From **Figure 6,** higher electrical resistivity is achieved with a lower W/C ratio. In addition, the non-proprietary UHPCs with RGP achieved a slightly higher electrical resistivity as compared with both the commercial UHPCs. Otherwise, the trend in increasing the resistivity over time has been very similar for all for different UHPCs.

Conclusion

Following conclusion can be drawn from this research:

1. Non-proprietary UHPC with recycled glass powder can be designed following a particle size distribution based on the modified A&A with a q-value of 0.22 to achieve compressive strength of 156 MPa to 178 MPa without the use of special treatment.
2. The fiber reinforced UHPC obtained tensile strengths up to 15 MPa (2.2 ksi) with multiple hairline cracks showing distinct strain hardening property before crack opening.
3. The cost of UHPC can be obtained in around US$550/m^3 without fibers and in between US$800 to US$1140/m^3 with the use of fibers available in the US.
4. The carbon footprint (*CFP*) is around 620 kg/m^3 for UHPC paste and in between 660-800 kg/m^3 for UHPC without fiber.
5. All non-proprietary UHPCs surpassed the low permeability threshold just in few days after casting.

Acknowledgement

This research is funded by the Transportation Infrastructure Durability Center at the University of Maine under grant 69A3551847101 from the U.S. Department of Transportation's University Transportation Centers Program. The authors would like to acknowledge the support from the Connecticut Department of Transportation (CTDOT) and the Advanced Cementitious Materials and Composites (ACMC) lab at the University of Connecticut. The authors would also like to thank all the material suppliers: LafargeHolcim, Ferroglobe PLC, Urban Mining Northeast, Tilcon, Chryso Inc., Bekaert, and Steelike.

References

"AASHTO-T95 Standard Test Method for Surface Resistivity of Concrete's Ability to Resist Chloride Ion Penetration." *American Association of State Highway and Transportation Officials*, 2014, p. 10.

ASTM C109. *Standard Test Method for Compressive Strength of Hydraulic Cement Mortars (Using 2-in. or [50-Mm] Cube Specimens)*. 2002.

ASTM C230. *Standard Specification for Flow Table for Use in Tests of Hydraulic Cement*. 2008, www.astm.org.

ASTM C1866. *Standard Specification for Ground-Glass Pozzolan for Use in Concrete*. 2020, https://doi.org/10.1520/C1866_C1866M-20.

Dyer, Thomas D., and Ravindra K. Dhir, 2001. *CHEMICAL REACTIONS OF GLASS CULLET USED AS CEMENT COMPONENT*.

Kaminsky, Amanda, et al., 2020 *Ground-Glass Pozzolan for Use in Concrete*., www.vitrominerals.com.

Omran, Ahmed, et al., 2018. "Performance of Ground-Glass Pozzolan as a Cementitious Material-a Review." *Advances in Civil Engineering Materials*, vol. 7, no. 1, 2018, pp. 237–70, https://doi.org/10.1520/ACEM20170125.

Sakai, E., et al. 2008. "Influence of Superplasticizer on the Fluidity of Cements with Different Amount of Aluminate Phase." *Second International Symposium on Ultra High-Performance Concrete*, 2008, pp. 85–92.

Soliman, N. A., and A. Tagnit-Hamou. 2016."Development of Ultra-High-Performance Concrete Using Glass Powder – Towards Ecofriendly Concrete." *Construction and Building Materials*, vol. 125, Oct. 2016, pp. 600–12, https://doi.org/10.1016/j.conbuildmat.2016.08.073.

Soliman, N. A., and A. Tagnit-Hamou. 2017. "Partial Substitution of Silica Fume with Fine Glass Powder in UHPC: Filling the Micro Gap." *Construction and Building Materials*, vol. 139, May 2017, pp. 374–83, https://doi.org/10.1016/j.conbuildmat.2017.02.084.

Soliman, Nancy A., and Arezki Tagnit-Hamou. 2017. "Using Glass Sand as an Alternative for Quartz Sand in UHPC." *Construction and Building Materials*, vol. 145, Aug. 2017, pp. 243–52, https://doi.org/10.1016/j.conbuildmat.2017.03.187.

Tohoué Tognonvi, Monique. 2018. "Reactivity of Glass Powder in Aqueous Medium." *Advances in Materials*, vol. 7, no. 1, 2018, p. 9, https://doi.org/10.11648/j.am.20180701.12.

Urban Mining, 2019. *Performance of Pozzotive ® with McInnis PLC*. 2019.

Urban Mining Northeast, 2020. *Technical Brief: Pozzotive® Chloride and Sulfate Blockers*. 2020.

Vaitkevičius, Vitoldas, et al. 2014. "The Effect of Glass Powder on the Microstructure of Ultra High Performance Concrete." *Construction and Building Materials*, vol. 68, Oct. 2014, pp. 102–09, https://doi.org/10.1016/j.conbuildmat.2014.05.101.

Wille, K., et al. 2013. "Properties of Strain Hardening Ultra High Performance Fiber Reinforced Concrete (UHP-FRC) under Direct Tensile Loading." *Cement and Concrete Composites*, vol. 48, Apr. 2014, pp. 53–66, https://doi.org/10.1016/j.cemconcomp.2013.12.015.

Wille, K., et al. 2011. "Ultra-High-Performance Concrete with Compressive Strength Exceeding 150 MPa (22 Ksi): A Simpler Way." *ACI Materials Journal*, vol. 108, no. 1, Jan. 2011, pp. 34–46.